

## Round robin study on spectral fatigue assessment of butt-welded joints

J. Rörup

*DNV GL—Maritime, Hamburg, Germany*

Y. Garbatov, Y. Dong & E. Uzunoglu

*CENTEC, Universidade de Lisboa, Portugal*

G. Parmentier & A. Andoniu

*Bureau Veritas Marine, Paris, France*

Y. Quéméner & K.-C. Chen

*CR Classification Society, Taipei, Taiwan*

S. Vhanmane, A. Negi & Y. Parihar

*Indian Register of Shipping, Mumbai, India*

R. Villavicencio & V. Parsoya

*Lloyd's Register, GTC Southampton, UK*

L. Peng & J. Yue

*Wuhan University of Technology, Wuhan, China*

**ABSTRACT:** The objective of this study is to perform a round robin study on spectral fatigue damage assessment of butt-welded joints and to identify the existing uncertainties and challenges in the commonly used approaches. Various methods are employed to estimate the fatigue damage of butt-welded joints located in the deck and shell structure of a bulk carrier. Hydrodynamic loads are calculated based on strip and panel theory and closed form hydrodynamic loads. The finite element method and beam theory are both feasible to calculate the stress responses and the analysis procedures for each method are introduced and the corresponding results are compared and conclusion are derived.

### 1 INTRODUCTION

The most accurate way of fatigue life estimation in practice today is the spectral approach, which simulates the time history of ship structural response in waves by a linear superposition. The basis for developing loads in the spectral analysis method is the development of transfer functions generally referred to as Response Amplitude Operators, or RAO's. RAO represents the response of the ship's structure to excitation by a wave of unit height, and it is derived over the full range of (encounter) frequencies that will be experienced. RAO's express the amplitude and phase relationship between the wave load and the response.

The frequency response of the load components is determined by hydrodynamic analysis. Different numerical hydrodynamics methods have been developed.

First methods were based on a 2D-theory and used a velocity potential with linear assumptions only. To compensate the insufficient solution of strip theory in long waves and of slender hulls in short waves a unified theory was developed (Maruo 1970, Newman & Sclavounos 1980, Kashiwagi, 1995). This 2D-seakeeping analysis yields good results, but cannot completely represent the 3D problem of a ship in waves.

Consequently, 3D boundary element methods were developed, using either a wave Green's function or a Rankine source in frequency or time domain.

Green function methods discretize the wetted hull surface into many small surface elements (panels). For each panel, a Green function defines the velocity potential. For numerical scheme and related problems with the Green's function, refer to Inglis & Price (1982), Iwashita & Ohkusu (1992) and Takaki, Iwashita & Lin (1992).

Only the Rankine method includes the potential for steady flow. In addition, more complicated boundary conditions on the free surface and the hull are considered. However, the free surface surrounding the hull as well as the hull itself must be discretized by panels. This method originally was applied successfully to the wave-ship interaction problem by Nakos (1989) Sclavounos & Nakos (1990). A comprehensive overview of various Rankin singularity methods for seakeeping is documented by Bertram & Yasukawa (1996).

For fatigue investigations, the ship response to the relevant wave excitation is linear and accordingly the response in a seaway is described by a superposition of the responses to all regular wave components that constitute the irregular sea, which can be performed in a frequency domain analysis. Given the linearity, the response is described by a stationary and ergodic, but not necessarily narrow-banded Gaussian process.

The stress transfer functions (RAOs) were evaluated directly from structural analysis with finite element method (FEM) or by simple beam models for selected fatigue locations. Stress range is normally expressed in terms of probability density functions for different short-term intervals corresponding to the individual cells of the wave scatter diagram. The linear addition of short term damages sustained over all sea states gives the total fatigue damage for the structural detail. Fatigue damage is calculated on the Palmgren-Miner approach and accumulated over operational service life by accounting for all sea states encountered.

This paper presents a round robin study on fatigue damages for transverse butt welds in the upper hull of a bulk carrier. Considering an axial misalignment of 10% in plate thicknesses a ‘FAT80’ was employed by all participants for the nominal stress approach. Thickness effect was considered from all participants in the same way, here exists a common understanding by all applied class rules. Mean stress effects were considered individually according to the applied classification rules. For the hydrodynamic analysis and statistical approach, all participants use following unified input parameters:

- wave lengths  $\lambda$ , 25 to 1125 m,  $\Delta\lambda = 50$  m
- wave directions  $\Theta$ , 0 to 360°,  $\Delta\Theta = 30^\circ$
- 75% of service speed, ~11 knots
- directional spreading ( $\cos, n = 2$ )
- wave spectrum: Pierson-Moskowitz form
- long term scatter diagram: World-wide
- service life: part of life at sea: 0.85\*25 years
- uniform weighting factors for heading angles

The round robin study was carried out to identify existing challenges in commonly used fatigue spectral approaches as part of the “Fatigue and

Fracture” committee at ISSC 2018. Seven institutes participated in the round robin study with nine different approaches. Ship data of the investigated Suez-max bulk carrier, a global FE-model and nodal forces representing the mass distributions of four loading conditions were offered to the participants.

The participants were requested to assess fatigue damage for transverse butt welds at two x-positions in the mid ship area, for each at three different locations in the upper hull. Beside the fatigue damages, a comparison of the RAO’s and long-term values for vertical bending moment was carried out, too.

## 2 SHIP DATA

A bulk carrier design with a double hull side structure was chosen as target ship for the round robin study. Principal dimensions of the bulk carrier are given in Table 1. The fatigue life of transverse butt welds in the upper hull of a bulk carrier is investigated. Two frame locations are chosen, see Figure 1. One in hold 6, the heavy ballast hold and the other in hold 5, which is a loaded hold in alternate condition. Fatigue damage will be computed for each x-position at three different locations, see Figure 2.

Hull girder cross section properties at the two investigated x-locations, based on the gross and net50 scantlings, were distributed to the participants.

### 2.1 Loading conditions

The spectral fatigue assessment was conducted for four loading conditions, namely:

Table 1. Principal dimensions of the bulk carrier.

Length	~285 m
Breadth	~47 m
Depth	~25 m
Draft	~17 m

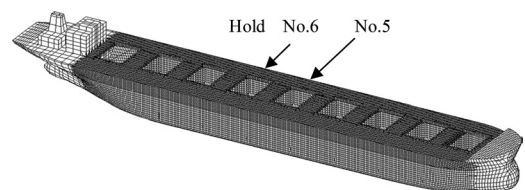


Figure 1. Finite element model of the bulk carrier.

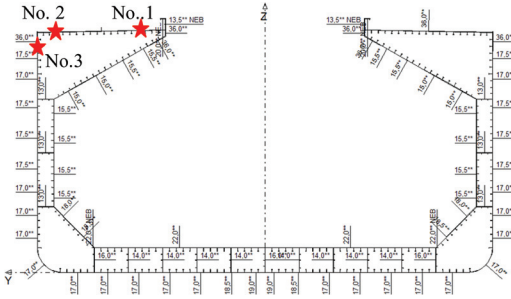


Figure 2. Cross section of hold 5 at  $x/L = 0.55$ .

Table 2. Still water bending moments.

Condition	SWBM in $10^6$ [kNm]		Fraction of time
	at $x/L = 0.45$	at $x/L = 0.55$	
Homogenous	-1.316	-1.530	0.25
Alternate	3.272	2.057	0.25
Normal Ball.	2.969	2.803	0.20
Heavy Ball.	-1.660	0.365	0.30

- *Homogeneous* full load departure condition, all cargo holds filled with cargo of density  $0.9 \text{ t/m}^3$ . All wing and double bottom water ballast tanks empty.
- *Alternate departure* condition loaded with a cargo of density  $3 \text{ t/m}^3$  in hold 1, 3, 5, 7 and 9. All wing and double bottom water ballast tanks empty.
- *Normal Ballast* departure condition, double wing and bottom tanks filled with 70,000 t water ballast. All cargo holds empty.
- *Heavy Ballast* departure condition, all, double wing and bottom tanks filled with  $\sim 75,000$  t water ballast. Cargo hold No.6 filled with  $\sim 22,000$  t ballast water.

Drafts, centre of gravity, GM-values, Radii of Gyration, displacements and block coefficients of the investigated loading conditions were distributed to the participants.

Table 2 shows the still water bending moments at the two relevant  $x$ -positions and considered the fraction of time in operation for all loading conditions.

### 3 PARTICIPANTS AND THEIR METHODS

Seven institutes participated in the round robin study with nine different approaches in total. For each participant, the applied hydrodynamic

software is shortly introduced. For the homogeneous loading condition, each member demonstrates his hydrodynamic results for vertical bending moment by a RAO diagram. Furthermore, the way of stress determination and if relevant, the mass application in the global FE-model is explained.

#### 3.1 Method of DNV GL

With DNV GL software ShipLoad all masses were applied directly on the structural model and resulting nodal forces in the FE model reproduced the total mass of the ship, including the mass of structure, equipment, engine etc. Tank liquid and cargo masses are reproduced by nodal forces, too, considering the hydrostatic pressure distribution on all tank and cargo hold boundaries. With this mass distribution in the global FE-model the hydrodynamic calculations are conducted and are used later for stress determination, too. The hydrodynamic potentials are determined by a 3-D Rankine code. The fatigue approach was carried out according to DNV GL (2015a, b).

#### 3.2 Method of CENTEC

The 2-D linear strip theory is employed to estimate the hydrodynamic loads among which only

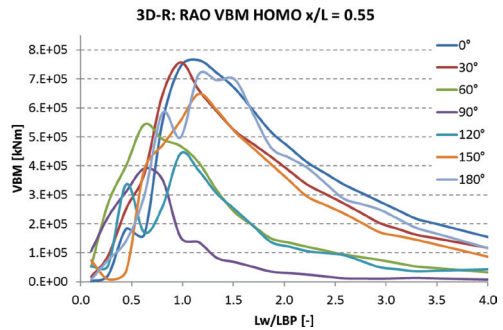


Figure 3. RAO's for VBM from DNV GL.

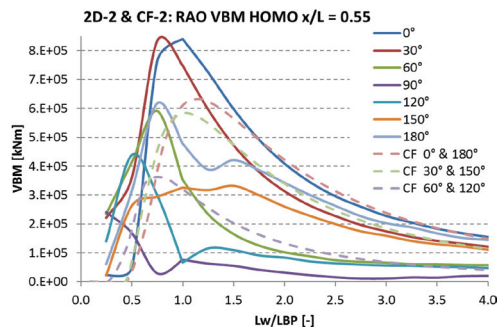


Figure 4. RAO's for VBM from CENTEC.

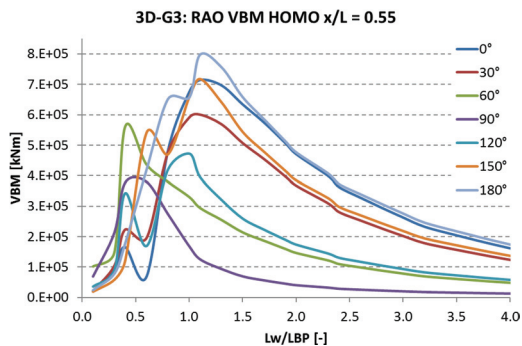


Figure 5. RAO's for VBM from BV.

the wave-induced vertical bending moment is taken into account. In this case, the global finite element method is used to determine the stress load ratios and static stresses at the locations of interest.

As an alternative to the 2-D linear strip theory a parametric approach, developed by Jensen & Mansour (2002) for specific vessel types and loads, is also employed here. The stress load ratios and static stresses are calculated based on the beam theory.

### 3.3 Method of Bureau Veritas (BV)

The spectral fatigue assessment has been carried out according to BV's guidelines NI611, Bureau Veritas (2016) based on stress RAOs obtained using the global FE model of the ship. The lightship weight was modeled by means of nodal masses derived from the available nodal forces. Liquid ballast was taken into account by directly modeling the ballast tanks for which the radiation problems are solved in order to obtain pressures on the tank boundaries. Finally, dry cargo is modeled by means of nodal masses placed at the indicated center of gravity and inertia loads are distributed on the boundaries of the cargo hold.

BV's software Homer v2.1.4 was used to perform the coupled hydro-structure analysis. The hydrodynamic coefficients for both the hull and ballast tanks are calculated using the 3D-Green function potential flow code Hydrostar v7.3. Pressures are then computed at the FE mesh points and integrated over the FE mesh which ensures an implicit balance between the inertia loads and hydrodynamic and hydrostatic forces. Finally, structural analysis is performed in order to determine the stress RAOs at the locations of interest.

### 3.4 Method of CR classification society

The coupled hydro-structure analyses were conducted using Homer 1.2 from Bureau Veritas (BV). The finite element model of the ship struc-

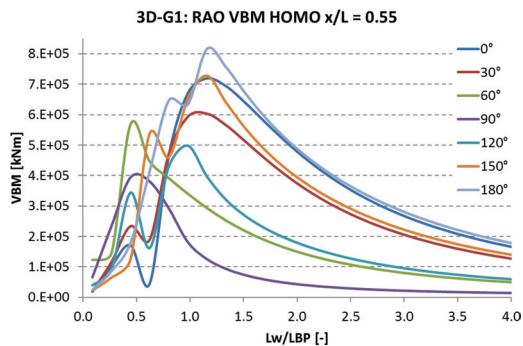


Figure 6. RAO's for VBM from CR.

ture included nodal masses to reproduce the dry cargo and water ballast inertia loads that were distributed to the hold/tank boundaries using NX Nastran's rigid body elements (RBE3).

The seakeeping analyses were carried out using Hydrostar 7.25 (BV), a 3-D-Green-Function potential flow code. The hydrodynamic pressures were then transferred on the structural mesh elements, and the ship motion accelerations were applied to balance the model. The finite element analyses were then conducted for each combination of wave frequency and heading by NX Nastran, and the RAOs of stress were extracted at the considered hot spots. The conversion to fatigue hot spot stress RAO was conducted accordingly to the CSR (IACS, 2015).

### 3.5 Method of Indian Register of Shipping (IRS)

Fatigue assessment is based on two methods (2-D strip and closed form) to compute nominal stress. Consideration is given to global loads (vertical and horizontal bending moments). However, the closed form method considers only vertical bending moment (Jensen & Mansour, 2002).

The beam theory is employed to obtain the nominal stresses for the given welded joints. Spectral analysis is performed accounting the appropriate mean stress effect, thickness factor (reference thickness is assumed as 25 mm) and rain flow correction factor (Wirching & Light, 1980). A suitable bi-linear S-N curve is selected for given structural details.

### 3.6 Method of Lloyds Register (LR)

The Lloyd's Register (LR) software WaveLoad-FD is used for the hydrodynamic analysis, which uses the Green function for computing the hydrodynamic potentials. In the hydrodynamic analysis, the mass distribution is determined with the LR software ShipRight where the cargo and ballast

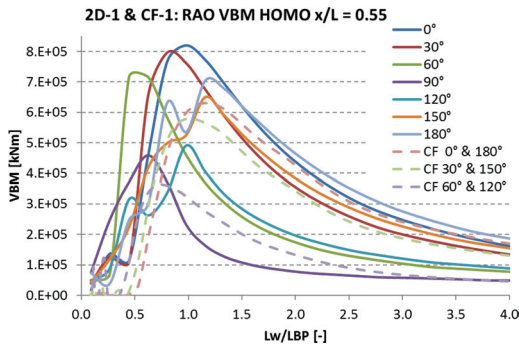


Figure 7. RAO's for VBM from IRS.

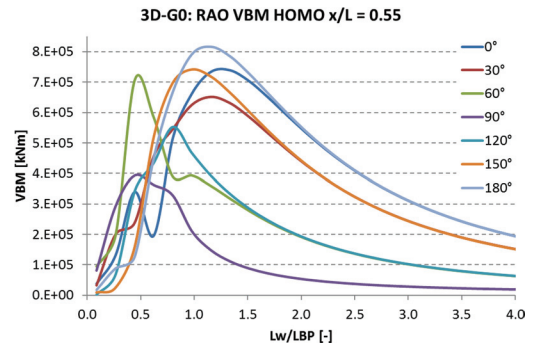


Figure 9. RAO's for VBM from WHUT.

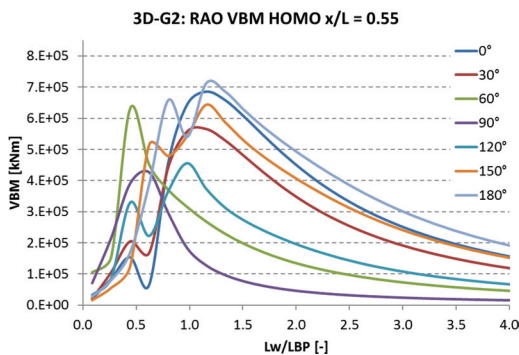


Figure 8. RAO's for VBM from LR.

tanks, as well as other compartments, are automatically detected and then the respective loading is assigned as per the loading manual.

The fatigue assessment uses the three-hold finite element model (holds 4, 5 and 6) and follows LR procedures (LR 2016a). The loading of the model and the combination of the stresses is carried out using the LR software ShipRight (LR 2016b). ShipRight adopts a unit load approach to estimate the total stress response by combining the results of discrete unit load cases and the applied loads.

The unit cases include hull girder global loadings, external hydrodynamic wave pressure loads, and internal solid cargo/water ballast inertia pressure loads. All these loads are further computed for any loading condition and sea state resulting from the hydrodynamic analysis and scatter diagram. The distribution and magnitude of the internal inertia pressure loads are determined by simplified expressions for each ship motion.

### 3.7 Method of Wuhan University (WHUT)

Hydro model was built according to the hull of the bulk carrier. Hydrodynamic loads were determined

Table 3. Summary of methods.

	Hydro code	Stresses from	Fatigue rules
DNVGL	3D- Rankine	Global FE	DNVGL
CR	3D-Green-func.	Global FE	CSR
LR	3D-Green-func.	Cargo Hold FE	LR
BV	3D-Green-func.	Global FE	BV
IRS	2D-Strip	Beam, V&H BM	IRS
	Closed Form	Beam, VBM	IRS
CENTEC	2D-Strip	Global FE, VBM	DNVGL
	Closed Form	Beam, VBM	DNVGL
WHUT	3D-Green-func.	Global FE	DNV

based on the Green function and wave induced forces for a specified set of wave frequencies and heading angles were obtained by the DNVGL software SESAM. Wave loads were mapped from the panels to the hull elements in the global model, which indicated that all loads effects would be involved in SFA.

The FE analysis was based on the Classification Note No. 30.7 from DNV. With the Palmgren-Miner approach, the accumulated fatigue damage of six hot spots in each loading condition was calculated. It should be noted that only the responses in zero speed were considered in the analysis.

### 3.8 Summary of methods

Table 3 summarizes the applied methods from all participants.

## 4 COMPARISON OF RESULTS

### 4.1 Response amplitude operators

The vertical bending moment represents the primary load component for the investigated details. By example, the RAO's for the homogenous load-

ing condition at  $x/L = 0.55$  are shown for each participant in Figures 3 to 9. The maximum values in the head or following seas are in the range of 710,000–840,000 kNm/m. An exception exists for the closed form solution in Figs. 4 and 7 where the VBM is only of 610,000 kNm/m. For all the loading conditions, the closed form predictions represent either the lower or the upper bound of the VBM values produced by all the participants (see also long-term values in Figs. 10 to 13).

For direct investigated RAO's the differences in aft-oblique sea are much more present than in other heading angles. Particularly for a heading angle of  $60^\circ$ , occurs here in some cases a pitch resonance and results in a high VBM. For  $90^\circ$ – $150^\circ$  heading angle, this phenomenon does not exist and the results scatter less than in aft-oblique sea.

#### 4.2 Long-term values

The long-term values of the vertical bending moment were assessed through spectral analysis by

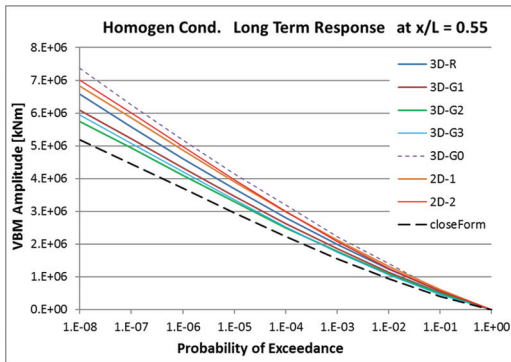


Figure 10. Long-term values for VBM in Homogen Condition.

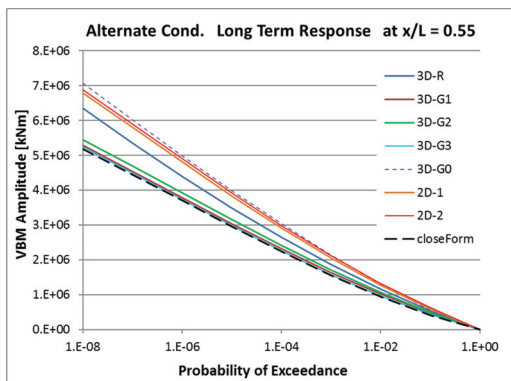


Figure 11. Long-term values for VBM in Alternate Condition.

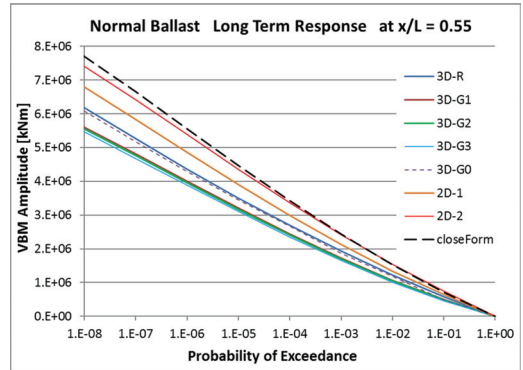


Figure 12. Long-term values for VBM in Normal Ballast.

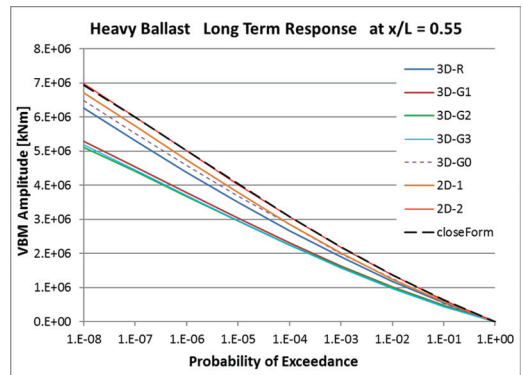


Figure 13. Long-term values for VBM in Heavy Ballast.

all participants using their own investigated RAOs or from closed form and following settings:

- Pierson-Moskowitz wave spectrum,
- Angular spreading of wave energy by  $\cos^2$ -funct.,
- Equal heading probability, and
- World-wide wave scatter diagram

Figures 10 to 13 present the long-term values of VBM for each loading condition. By trend, the long-term values of VBM produced by 2D-seakeeping analyses are higher than those obtained by 3D methods. For the long-term values of all participants (without closed form) exist a maximum deviation of about 30% for all conditions and probability levels.

In Table 4 the fatigue interesting long-term values of the  $10^{-2}$  probability level are listed for all methods and loading conditions.

Application of the hydrodynamic closed form solution results always in an imprecise forecast. For all loading conditions, the closed form solutions

Table 4. 10-2 long-term value of VBM at  $x/L = 0.55$ .

$10^6$ [kNm]	Homogen loaded	Alternate loaded	Normal Ballast	Heavy Ballast
3D-R	1.244	1.156	1.222	1.188
3D-G1	1.143	1.018	1.069	1.016
3D-G2	1.095	1.059	1.052	0.997
3D-G3	1.058	0.951	1.057	0.988
2D-1	1.319	1.270	1.342	1.250
CF-1	0.934	0.934	1.526	1.293
2D-2	1.265	1.330	1.542	1.363
CF-2	0.990	0.990	1.560	1.367
3D-G0	1.407	1.309	1.192	1.275

either represent the lower or upper bound in the scatter of all results.

### 4.3 Fatigue damage

For this benchmark study, the fatigue life of transverse butt-weld connections amidship in the upper hull were assessed using the nominal stress approach. Considering an axial misalignment of 10% in plate thicknesses 'FAT80' was applied for the fatigue investigation from all participants.

The fatigue damages on the Palmgren-Miner approach were directly calculated through a spectral analysis using the nominal stress RAOs on which were applied correction factors that include the effect of corrosion, mean stress and thickness effect. These factors were determined according to the applied class rules. Clear differences exist for the mean stress. By example Table 5 shows for the location No.2 at  $x/L = 0.55$  the applied mean stress factor for all four loading conditions.

Figure 14 shows for the location No.2 at  $x/L = 0.55$  the fatigue damages for the different loading conditions and the combined one. Although for a single loading condition obvious differences exist due to hydrodynamic inputs and mean stress effects, the combined damages are on a comparable level for all approaches. In case of an approach with RAOs from the closed form, the Normal Ballast conditions contribute much more than the other loading conditions, particularly the two loaded conditions have a much lower contribution.

The combined fatigue damages for all investigated locations are shown in Figure 15. The differences in fatigue damages for the combined case are reduced in comparison with single loading conditions. The approaches CF-1, 2D-2 and CF-2 that consider only the vertical bending moment for the stress assessment, indicate always the location P1 as the most critical for both cross sections because P1 is at the largest vertical distance to the ship section

Table 5. Correction factors for mean stress effect.

	Homogen loaded	Alternate loaded	Normal Ballast	Heavy Ballast
3D-R	0.810	0.969	1.000	0.911
3D-G1	0.612	0.976	1.000	0.918
3D-G2	1.000	1.000	1.000	1.000
3D-G3	1.000	1.000	1.000	1.000
2D-1	0.839	1.000	1.000	0.927
CF-1	0.807	1.000	1.000	0.928
2D-2	0.781	0.941	0.976	0.894
CF-2	0.751	0.984	0.969	0.867
3D-G0	0.893	0.963	0.994	0.903

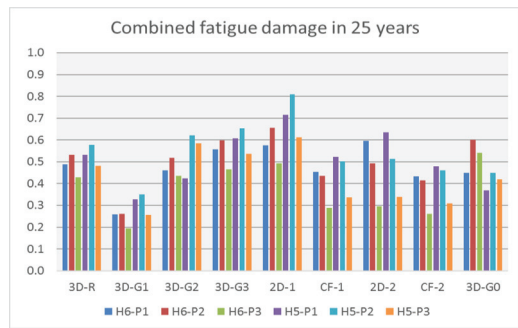


Figure 14. Fatigue damages for location No.2 at  $x/L = 0.55$ .

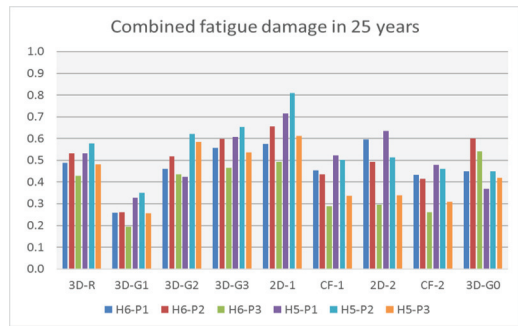


Figure 15. Combined fatigue damages for all locations.

neutral axis. All other approaches that employ a direct stress assessment from the FE model loaded accordingly to the hydrodynamic analyses results, indicate always the location P2 as the most critical. The direct stress assessment approach is more precise because it allows for considering further hull girder load components and possible local bending effects.

## 5 CONCLUSIONS

The work presented here performed a round robin study on the spectral fatigue damage assessment of butt-welded joints employing various methods to estimate the fatigue damage of butt-welded joints located in the deck and shell structure of a bulk carrier. Hydrodynamic loads were calculated based on strip and panel theory and closed form hydrodynamic loads. The finite element method and beam theory demonstrated to be feasible in estimating the ship hull stress responses.

Since wave-induced loads are the most significant contributing factor to fatigue, the outcomes of the ship motion and load analysis will determine the fatigue damage of the butt-welded joints. All participants used the same inputs for their hydrodynamic analyses. However, the methods to compute the hydrodynamic potentials differ among them. By trend the long-term values of VBM are higher from 2D-seakeeping analysis than from 3D-methods. The application of the hydrodynamic closed form solution results in an imprecise forecast, as it either represents the lower or the upper bound in the scatter of all results and for all loading conditions.

It has been noticed that the horizontal bending and torsion have a moderate impact with following effect on the fatigue results: The assessment methods that only consider the vertical bending moment effect predict that the location P1 close to the hatch coaming is the most critical. On the other hand, when considered further hull girder load components and possible local bending effects, the other approaches indicate that the location P2 is the most critical.

Although all loading conditions exhibit obvious differences in the fatigue damage, mainly due to the different hydrodynamic loads and mean stress effects, the combined damage is comparable at a certain level.

## REFERENCES

Bertram V. and Yasukawa H. (1996). Rankine Source Methods for Seakeeping Problems. *Jahrbuch Schiffbautechnische Gesellschaft*, Vol. 90, pp. 411–425.  
Bureau Veritas. (2016). NI 611 Guideline for Fatigue Assessment of Steel Ships and Offshore Units. BV.

DNV GL (2015a). DNVGL-RU-9111:2015-7, “Rules for Classification, Part 3 Hull, Chapter 9 Fatigue”, DNV GL, Oslo.  
DNV GL (2015b). Class Guideline DNVGL-CG-0129: “Fatigue Assessment of Ship Structures”, DNV GL, Oslo.  
IACS (2015). “Common Structural Rules for Bulk Carriers and Oil Tankers”, International Association of Classification Societies, London.  
Inglis R.B. & Price, W.G. (1981). A Three-Dimensional Ship Motion Theory; Comparison between Theoretical Predictions and Experimental Data of the Hydrodynamic Coefficients with Forward Speed. *Trans. RINA*, 124.  
Iwashita H. & Ohkusu M. (1992). Green Function Method for Ship Motions at Free Speed, *Ship Technology Research*, 32, 2.  
Jensen JJ. & Mansour AE. (2002). Estimation of ship long-term wave-induced bending moment using closed-form expressions. *Royal Institution of Naval Architects Transactions Part A International Journal of Maritime Engineering*.  
Kashiwagi M. (1995). Prediction of Surge and its Effect on Added Resistance by Means of the Enhanced Unified Theory. *Trans. West-Japan Society of Naval Architects*, 89, pp. 77–89.  
LR (2016a). *ShipRight Design and Construction: Fatigue Design Assessment – Application and Notations (Notice 1 and Notice 2)*. Lloyd’s Register Group Limited, London, UK.  
LR (2016b). *ShipRight Design and Construction: Fatigue Design Assessment – Level 3 Procedure Guidance on Direct Calculations (Notice 1)*. Lloyd’s Register Group Limited, London, UK.  
Maruo H. (1970). An improvement of the Slender Body Theory for Oscillating Ships with zero Forward Speed. 19. *Bulletin of the Faculty of Engineering, Yokohama National University*, pp. 45–66.  
Nakos D. (1989). Free surface methods for unsteady forward speed flows, *Proc. 4th Int. workshop on water wave and floating bodies, Norway*.  
Newman J.N. & Sclavounos P. (1980). The unified theory of ship motions. In: *Proc. of the 28th Symposium of Naval Hydrodynamics, Tokyo*.  
Sclavounos P. & Nakos D. (1990). Ship motions by Three-dimensional Rankine panel method. 18th *Symposium on Naval Hydrodynamics*.  
Takai M., Iwashita H. & Xin Lin. (1992). Forces on a ship with forward speed in waves, *Proc. Int. Ocean Space and resource utilization seminar and 29th ocean engineering research workshop, Ulsan, Korea*.  
Wirsching PH & Light MC (1980). Fatigue under wide band random stresses. *Journal of the Structural Division*. 1980; 106:1593–607.